Conservation of Magnetic Helicity during Plasma Relaxation

H. Ji,* S. C. Prager, and J. S. Sarff
Department of Physics, University of Wisconsin, Madison, Wisconsin 53706
(Received 9 July 1994)

The change in magnetic energy and magnetic helicity has been measured during the sawtooth relaxation in the Madison Symmetric Torus reversed-field pinch. The larger decay of the energy (4.0%–10.5%), relative to helicity decay (1.3%–5.1%), modestly supports the helicity conservation hypothesis in Taylor's relaxation theory. However, the observed helicity change is larger than the simple magnetohydrodynamics prediction. Enhanced fluctuation-induced helicity transport during the relaxation is observed.

PACS numbers: 52.30.Jb, 52.25.Gj, 52.55.Hc

Magnetic helicity [1] is a measure of the "knottedness" of magnetic field. It is an invariant within a flux tube in a perfectly conducting plasma. In 1974 Taylor conjectured [2] that in a "slightly" resistive plasma the *total* helicity is well conserved during plasma relaxation in which the magnetic energy decays toward a minimum-energy state. This well-known hypothesis has been successful [2] in explaining magnetic structures in laboratory plasmas, such as the reversed-field-pinch (RFP), spheromak, and multipinch. It has also been applied to relaxation in tokamak [3,4], magnetospheric [5], and solar [6] plasmas. The conjecture has been extended theoretically [7] and studied through nonlinear MHD computations [8–11]. However, to our knowledge, this rather well-accepted conjecture has received little experimental test. Helicity conservation has been inferred by applying the helicity balance equation to a spheromak [12] and in the RFP [13].

In this Letter, we report an experimental investigation of the magnetic helicity and energy evolution during plasma relaxation in the Madison Symmetric Torus (MST) RFP. The test of Taylor's conjecture is possible since relaxation occurs in the MST as events which are discrete in time (corresponding to the 100 μs crash phase of a sawtooth oscillation). We find that during the relaxation event the magnetic helicity decreases by 1.3–5.1 %, while the magnetic energy decreases by 4.0–10.5 %. (Smaller helicity decay corresponds to smaller energy decay.) Hence the helicity conservation conjecture is modestly well satisfied in that the helicity decay is less than the energy decay by a factor of 2–3. Interestingly, the relatively violent sawtooth crash only dissipates a small fraction of the magnetic energy (presumably constrained by the relative conservation of helicity). However, the helicity decay is greater than that expected from simple resistive MHD arguments.

The gauge-invariant definition of the total helicity in a toroidal plasma is given by [14] $K \equiv \int \boldsymbol{A} \cdot \boldsymbol{B}\, dV - \Phi_\phi(a)\Phi_\theta(a)$ where $\boldsymbol{A}$ is the vector potential, $\boldsymbol{B}$ is the magnetic field, $\Phi_\phi(a)$ is the total toroidal flux, $\Phi_\theta(a)$ is the poloidal flux threading the central hole of the torus, and the integration is over the plasma volume. Taylor evaluated [2] a relaxed state by minimizing the magnetic energy $W = \int (\boldsymbol{B}^2/2\mu_0) dV$, subject to the constraint of constant helicity. The resulting field satisfies the equation $\nabla \times \boldsymbol{B} = \lambda \boldsymbol{B}$, where the current to field ratio $\lambda \equiv \mu_0 \boldsymbol{j} \cdot \boldsymbol{B}/B^2$ is a spatial constant. The Bessel function solutions to this equation (referred to as the Bessel function model, BFM) approximate well the measured fields in the RFP, except that in experiments λ falls to zero at the edge.

The MST [15] is a large RFP device ($R = 1.50$ m, $a = 0.52$ m) with plasma current I_p up to 700 kA. The plasma is surrounded by a 5-cm-thick aluminum shell with one toroidal and one poloidal gap. The shell also acts as the vacuum vessel and a single-turn toroidal field coil. Magnetic energy and helicity enter through the gaps across which nonzero toroidal $V_\phi(a)$ and poloidal $V_\theta(a)$ voltages occur.

Sawtooth oscillations [16] in the MST consist of a fast crash phase and a slow recovery phase. The plasma rapidly relaxes towards its minimum energy state during the crash within 0.2 ms. This is illustrated by changes in two dimensionless parameters: the reversal parameter $F \equiv B_\phi(a)/(\Phi_\phi/\pi a^2)$ and the pinch parameter $\Theta \equiv B_\theta(a)/(\Phi_\phi/\pi a^2)$. Figure 1(a) displays $\Phi_\phi(a)$, F, Θ, and $V_\theta(a)$ during a sawtooth oscillation, where $I_p \approx 210$ kA and $V_\phi(a) \approx 20$ V. $\Phi_\phi(a)$ increases by ~8% and I_p increases by no more than 1.5% while F and

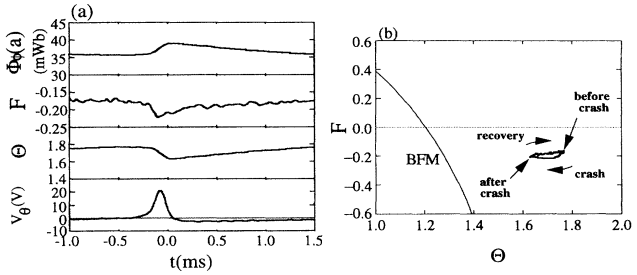

FIG. 1. (a) Ensemble-averaged toroidal flux $\Phi_\phi(a)$, pinch parameter Θ, reversal parameter F, and voltage across the toroidal gap in the shell $V_\theta(a)$ during one sawtooth cycle. The ensemble consists of 150 sawtooth oscillations. (b) Plasma trajectory during one sawtooth cycle. The BFM (Bessel function model) curve is the locus of predicted minimum energy states.

0031-9007/95/74(15)/2945(4)$06.00

Θ decrease during the crash. The increase in toroidal flux identifies the sawtooth crash as a "dynamo" field-generation event. The voltage across the toroidal gap in the shell, $V_\theta(a)$, serves later as a trigger for the sawtooth ensemble averaging and as a time reference. In Fig. 1(b), the trajectory in an F-Θ diagram approaches the minimum energy state (BFM curve) during the crash.

The important question here is whether the total helicity is conserved during the relaxation. The calculation of W and K requires knowledge of radial profiles of the magnetic field. ($\boldsymbol{A}$ is obtained by integrating $\boldsymbol{B} = \nabla \times \boldsymbol{A}$ over the radius.) Note that W and K are dominated by their mean-field values ($\boldsymbol{B}_0^2$ and $\boldsymbol{A}_0 \cdot \boldsymbol{B}_0$), with contributions from fluctuations ($\tilde{\boldsymbol{B}}^2$ and $\tilde{\boldsymbol{A}} \cdot \tilde{\boldsymbol{B}}$) smaller by a factor of 10^{-4}.

Lacking measurement of the magnetic field profiles, we deduce the profiles (and hence energy and helicity) from other measured quantities by employing equilibrium models. We find that the changes of K and W during a sawtooth crash can be accurately determined. First consider the "α model" [17] which assumes $\lambda = \lambda_0[(1 - (r/a)^\alpha]$ in $\nabla \times \boldsymbol{B} = \lambda \boldsymbol{B} + (\beta_0/2B^2)\boldsymbol{B} \times \nabla p$, where $\beta_0 \equiv 2\mu_0 p(0)/B^2(0)$ and $p(0)$ is the central plasma pressure. Every set of α, Θ_0 ($\equiv \lambda_0 a/2$), and β_0 with a specific pressure profile gives a unique prediction for F, Θ, and the central poloidal beta $\beta_{\theta 0}[\equiv 2\mu_0 p(0)/B_\theta^2(a)]$. Since F, Θ, and $\beta_{\theta 0}$ are measured quantities, it is possible to deduce the corresponding α, Θ_0, and β_0. To perform the inverse mappings, we have developed an artificial neural network (ANN) [18], trained by the error backward propagation technique [18] using a table created by forward mapping. The ANN has been shown to map (F, Θ, and $\beta_{\theta 0}$) to (α, Θ_0, and β_0) space with negligible errors.

From the dimensionless parameters (α, Θ_0, and β_0) and one dimensional parameter, say $\Phi_\phi(a)$, the helicity K and energy W can be obtained. The results with a parabolic pressure profile over the ensemble-averaged sawtooth oscillation are shown in Fig. 2. Other pressure profiles yield negligible differences. Both K and W decrease during the sawtooth crash, but the drop in W ($\simeq$8%) is considerably larger than in K ($\simeq$3%).

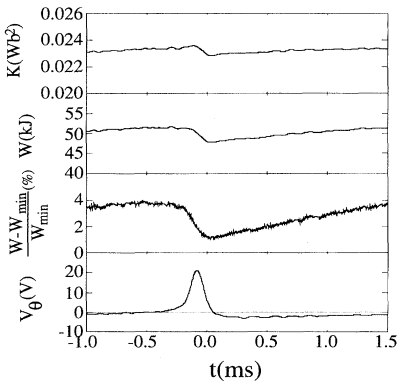

FIG. 2 The magnetic helicity K, magnetic energy W, and "excess energy" $(W - W_{\min})/W_{\min}$ during one sawtooth cycle. $W_{\min}$ is energy predicted by the BFM with a given K and $\Phi_\phi(a)$. Also shown is $V_\theta(a)$ as a time reference.

To determine the dependence of the results on the equilibrium model, three other models have been examined: the modified Bessel function model (MBFM) [19] with finite pressure, a smoothed MBFM, and the "2λ model." In the MBFM, λ is constant out to a cutoff radius r_b beyond which λ falls linearly to zero at the boundary. The smoothed MBFM has a more realistic rounded λ profile. In both models, the free parameters are r_b, Θ_0, and β_0. The 2λ model uses the λ value at the center, the λ value at $r/a = 0.8$, and β_0 as free parameters; it allows hollow λ profiles. The ANN again is trained for these three models. Table I compares results from all four models. The correction from toroidicity is approximated from the θ average of $2(\Lambda a \cos\theta/R)^2$, where Λ is the poloidal field asymmetry factor. From the measured Λ of $\simeq -0.1$ [20], the toroidal correction is about 0.1%. In all models, the helicity decreases by 3–4 % while the energy decreases by 7–9 % during the sawtooth crash. Taking into account the variations among models, the resulting helicity changes ranges from 1.3–5.1 %, corresponding to a 4.0–10.5 % change in W.

The change in W is in good accord with Taylor's theory. Given the helicity and toroidal flux, one can calculate the energy of the minimum energy state, $W_{\min}$, from the BFM. We find that W closely approaches $W_{\min}$ during the crash, i.e., the excess energy $(W - W_{\min})/W_{\min}$ decreases from 4% before the crash to 1% afterward (Fig. 2). The measured change of K of 1.3–5.1 % adheres less to the Taylor theory which assumed that K is invariant. However, the change in K is indeed less than that of W (by a factor of 2–3).

Another way to quantify the difference in dissipation rates is to compare the confinement times of the helicity and energy. The balance equations for K and W in a plasma bounded by a shell (with cuts) are given by

$$\frac{dK}{dt} = -2\int \boldsymbol{E} \cdot \boldsymbol{B}\, dV + 2\Phi_\phi(a)V_\phi(a), \quad (1)$$

$$\frac{dW}{dt} = -\int \boldsymbol{E} \cdot \boldsymbol{j}\, dV + I_\phi V_\phi(a) + I_\theta V_\theta(a), \quad (2)$$

where $\boldsymbol{E}$ is the electric field, $I_\phi \equiv I_p$, $I_\theta \equiv 2\pi R B_\phi(a)/\mu_0$, and the right-hand sides contain integral dissipation terms and input terms. We define confinement times for helicity $\tau_K = K/[2\Phi_\phi(a)V_\phi(a) - dK/dt]$ and for magnetic energy $\tau_W = W/[I_\phi V_\phi(a) + I_\theta V_\theta(a) - dW/dt]$. Between

TABLE I. Comparison of helicity K and relative changes $\Delta K/K$ and $\Delta W/W$ before and after a sawtooth crash for four different equilibrium models.

model	K_{before} (mW b²)	K_{after} (mW b²)	$\Delta K/K$ (%)	$\Delta W/W$ (%)
α model	23.58	22.84	−3.2	−7.7
MBFM	23.14	22.43	−3.1	−7.7
smoothed MBFM	23.31	22.61	−3.0	−7.6
2 − λ model	23.32	22.40	−4.0	−8.5

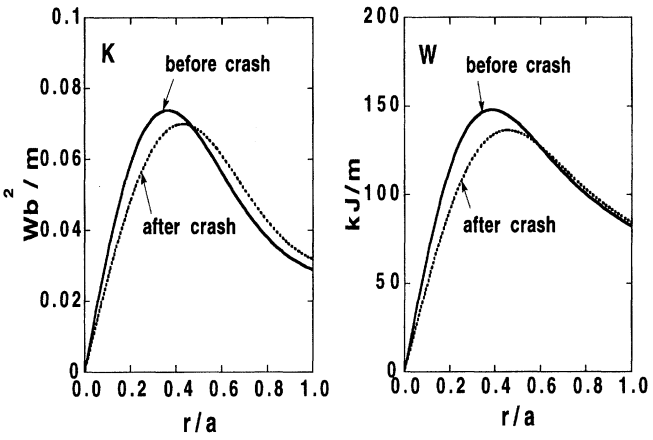

FIG. 3. Radial profiles of the helicity and energy per unit radial length before (solid line) and after (dotted line) the crash.

the crashes τ_K ($\simeq$21 ms) is comparable to τ_W ($\simeq$25 ms), but during the crash τ_K ($\simeq$3.4–7.8 ms) is longer than τ_W ($\simeq$1.9–4.2 ms) by a factor of 2–3.

Spatial information on the helicity and energy elucidates the transport properties. Figure 3 shows the helicity and energy per unit radial length before and after the crash. The magnetic energy largely decreases at the center with little increase at the edge, while the helicity apparently is transported from the center to the edge during the crash. This phenomenologically explains why the helicity is better conserved than energy.

Helicity transport is confirmed by local measurements of edge helicity flux due to fluctuations. The total helicity K can be split into three parts: core helicity in the $0 \le r \le b$ region, K_{core}, edge helicity in the $b \le r \le a$ region, K_{edge}, and the single linkage between edge poloidal flux and core toroidal flux, K_{link}. The balance equation for K_{edge} and K_{link} can be written as

$$\frac{dK_{\text{edge}}}{dt} + \frac{dK_{\text{link}}}{dt} = -2\int_b^a \eta \boldsymbol{j}_0 \cdot \boldsymbol{B}_0\, dV + 2\Phi_\phi(a)V_\phi(a) - 2\Phi_\phi(b)V_\phi(b) + 2\int \langle \tilde{\phi}\tilde{B}_r\rangle dS_b\,, \quad (3)$$

where η is Spitzer's resistivity and S_b is the surface area at $r = b$. The first term on RHS is deduced from $\boldsymbol{E} \cdot \boldsymbol{B} = \boldsymbol{E}_0 \cdot \boldsymbol{B}_0 + \langle \tilde{\boldsymbol{E}} \cdot \tilde{\boldsymbol{B}}\rangle$ by using the mean-field Ohm's law $\langle \tilde{\boldsymbol{E}} \cdot \tilde{\boldsymbol{B}}\rangle / B_0 = \eta j_0 - E_0$ verified experimentally in the MST edge [21]. The last term represents helicity transport across $r = b$ by correlation between fluctuations in plasma potential $\tilde{\phi}$ and radial field $\tilde{B}_r$ associated with dynamo activity. [Another helicity flux term $2\int \langle \tilde{A}_\theta (d\tilde{A}_\phi/dt)\rangle dS_b$ is small.]

The fluctuations $\tilde{\phi}$ and $\tilde{B}_r$ have been measured in the outer 5 cm region of the MST using a probe [21] containing both Langmuir probes and magnetic pickup coils. The measured fluctuation-induced helicity flux $\langle \tilde{\phi}\tilde{B}_r\rangle$ across the surface $r = b(= a - 5$ cm) shows that helicity is continuously transported to the edge between crashes and its flux is enhanced during the crash (Fig. 4). The other five terms in Eq. (3) have been measured (with η determined from T_e and estimated Z_{eff}) in the annular region during a sawtooth cycle. The predicted helicity flux from these five terms (the solid line in Fig. 4) agrees very well with the measured flux (dotted line). The enhanced helicity flux is balanced by the increases in $\dot{K}_{\text{edge}}$, $\dot{K}_{\text{link}}$, and ηjB by roughly the same magnitudes. Also, since the surface loss term [22] has been omitted in Eq. (3), the agreement implies that edge helicity dissipation, such as from limiters, is not important in the MST, unlike some other experiments [22].

The total helicity is predicted by MHD theory to be better conserved than we observe experimentally. The helicity balance [Eq. (1)] can be rewritten as

$$\frac{dK}{dt} = -2\int \eta \boldsymbol{j}_0 \cdot \boldsymbol{B}_0\, dV + 2\Phi_\phi(a)V_\phi(a) + 2\int \langle \tilde{\boldsymbol{v}} \times \tilde{\boldsymbol{B}}\rangle \cdot \boldsymbol{B}_0\, dV\,,$$

where the mean-field Ohm's law $\boldsymbol{E}_0 + \boldsymbol{v}_0 \times \boldsymbol{B}_0 + \langle \tilde{\boldsymbol{v}} \times \tilde{\boldsymbol{B}}\rangle = \eta \boldsymbol{j}_0$ has been used ($\boldsymbol{v}$ is the flow velocity). The first two terms on the RHS remain essentially unchanged during the crash. The last term has been predicted [23] to be small, as confirmed in MHD simulation [10], and to scale with resistivity as $2\int \langle \tilde{\boldsymbol{v}} \times \tilde{\boldsymbol{B}}\rangle \cdot \boldsymbol{B}_0\, dV \simeq -2\int \langle \eta \tilde{\boldsymbol{j}} \cdot \tilde{\boldsymbol{B}}\rangle dV$. By using $\tilde{j}/j_0 \le 1$ and $\tilde{B}/B_0 \lesssim 0.03$ in the MST, this term yields a helicity change of $\lesssim 0.03\%$ over the crash, which is smaller than the observed change by 2 orders of magnitude. This analytic estimate is consistent with MHD computation which displays sawtooth relaxations during which helicity drops by $\sim 6\%$ [11]. The Lundquist number S ($\propto \eta^{-1}$) of the simulations is 3×10^3, 200 times smaller than that in the MST. Therefore, the projected helicity change during a sawtooth crash in the MST is 200 times smaller, i.e., 0.03%. Hence the helicity should be well conserved in our experiments.

The helicity decay of 1.3–5.1 % during the crash implies a dissipation mechanism larger than that predicted

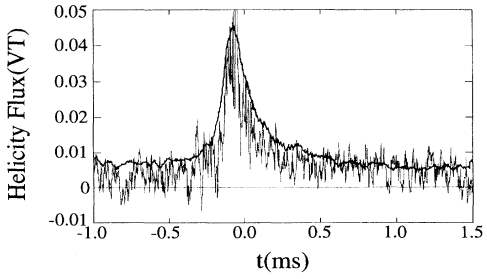

FIG. 4. Comparison between the measured fluctuation-induced helicity flux (dotted line) and the prediction (solid line) from local helicity balance at $r = a - 5$ cm.

TABLE II. Comparison of all terms in the helicity and energy balance equations, Eqs. (1) and (2), between and during the sawtooth crash.

	$\dot{K}$ (Wb^2/s)	$-2\int \boldsymbol{E}\cdot\boldsymbol{B}dV$ (Wb^2/s)	$2\Phi_\phi V_\phi$ (Wb^2/s)	$\dot{W}$ (MW)	$-\int \boldsymbol{E}\cdot\boldsymbol{j}dV$ (MW)	$I_\phi V_\phi + I_\theta V_\theta$ (MW)
Between crash	$0.2 \sim 0.6$	$-1.3 \sim -0.9$	1.5	$0.9 \sim 2.3$	$-2.7 \sim -1.3$	3.6
During crash	$-5.3 \sim -1.3$	$-6.9 \sim -2.9$	1.6	$-22.1 \sim -8.4$	$-24.9 \sim -11.2$	2.8

by a simple Ohm's law. Table II lists all three terms in Eqs. (1) and (2) between and during the crashes. Dissipation terms are enhanced by a factor of >2 for K and a factor of >4 for W during the crash, while the input terms remain essentially unchanged. Since dissipation at the edge is measured to be classical and its estimated enhancement during the crash can only account for less than 10% of the total helicity decrease, the anomalous dissipation must occur at the inner region. Possible candidates for the enhanced helicity dissipation are inferred by inserting the generalized Ohm's law [24] $\boldsymbol{E} = \eta\boldsymbol{j} - \boldsymbol{v}\times\boldsymbol{B} + \boldsymbol{j}\times\boldsymbol{B}/en - \nabla P_e/en$ into the helicity dissipation term to yield $\boldsymbol{E}\cdot\boldsymbol{B} = -\nabla P_e\cdot\boldsymbol{B}/en + \eta\boldsymbol{j}\cdot\boldsymbol{B}$. Volume integration of the first term may be rewritten as $-\int(\nabla n/en^2)P_e\boldsymbol{B}\,dV$. This term vanishes if P_e/n, or the electron temperature, is constant along the magnetic field. Considering the contribution of the fluctuating pressure, the term may be rewritten as $-\int(\nabla n/en^2)\langle\tilde{P}_e\tilde{B}_r\rangle dV$, where $\langle\tilde{P}_e\tilde{B}_r\rangle$ is identified as the electron momentum flux due to magnetic fluctuations (related to the kinetic dynamo mechanism [21]). From edge measurements of $\tilde{P}_e$ and $\tilde{B}_r$ we note that this term can be large. Other possible mechanisms of anomalous helicity dissipation may result from the kinetic modifications in the Ohm's law due to the fast electrons.

In summary, the first experimental test of Taylor's helicity conservation hypothesis has been performed during sawtooth relaxation in the MST RFP plasma. First, the observed substantial decay of the magnetic energy (4.0–10.5%) is in good accord with Taylor's relaxation theory. Second, the relatively smaller decay of helicity (1.3–5.1%) modestly supports the essence of the helicity conservation conjecture. However, the result that the decay ratio of energy to helicity is a factor of 2–3 instead of orders of magnitude, indicates that helicity conservation is only a rough approximation. Third, the helicity change is larger than the simple MHD prediction. Determination of detailed mechanisms for possible anomalous helicity dissipation during relaxation awaits further investigations. Fourth, enhanced transport of helicity, rather than local dissipation during the crash, phenomenologically explains its weaker decay, confirmed by a direct experimental observation of helicity flux due to the dynamo fluctuations. Finally, we note that the current investigation is based on equilibrium modeling; the direct, accurate determination of K and W from profile measurements remains an experimental challenge.

One of the authors (H. J.) thanks Professor K. Itoh and Professor S. I. Itoh for their encouragement and Professor Z. Yoshida for valuable discussions. The authors are grateful to the MST group, particularly Dr. A. Almagri, for their experimental contributions. This work was supported by the U.S. Department of Energy.

*Present address: Plasma Physics Laboratory, Princeton University, P.O. Box 451, Princeton, New Jersey 08543.

[1] H. K. Moffatt, J. Fluid Mech. **35**, 117 (1969).
[2] J. B. Taylor, Phys. Rev. Lett. **33**, 1139 (1974); Rev. Mod. Phys. **58**, 741 (1986).
[3] B. B. Kadomtsev, Sov. J. Plasma Phys. **1**, 389 (1975); F. L. Waelbroeck, Phys. Fluids **B1**, 2372 (1989).
[4] A. H. Boozer, Phys. Fluids **29**, 4123 (1986); Plasma Phys. Control. Fusion **36**, 825 (1994).
[5] Y. Song and R. L. Lysak, J. Geophys. Res. **94**, 5273 (1989).
[6] M. A. Berger, Geophys. Astrophys. Fluid Dyn. **30**, 79 (1984).
[7] For example, A. Bhattacharjee *et al.*, Phys. Rev. Lett. **45**, 347 (1980); Y. Kondoh, J. Phys. Soc. Jpn. **58**, 489 (1989).
[8] R. Horiuchi and T. Sato, Phys. Rev. Lett. **55**, 211 (1985).
[9] J. P. Dahlburg *et al.*, Phys. Rev. Lett. **57**, 428 (1986).
[10] Y. L. Ho, Ph.D. thesis, University of Wisconsin, 1988.
[11] K. Kusano and T. Sato, Nucl. Fusion **30**, 2075 (1990).
[12] C. W. Barnes *et al.*, Phys. Fluids **29**, 3415 (1986).
[13] K. Schoenberg *et al.*, Phys. Fluids **27**, 1671 (1984).
[14] M. K. Bevir and J. W. Gray, in Proceeding of the Reversed-Field Pinch Theory Workshop, Los Alamos, 1981, Report No. LA-8944-C.
[15] R. N. Dexter *et al.*, Fusion Technol. **19**, 131 (1991).
[16] S. Hokin *et al.*, Phys. Fluids **B3**, 2241 (1991).
[17] V. Antoni *et al.*, Nucl. Fusion **26**, 1711 (1986).
[18] B. Müller and J. Reinhardt, *Neural Network* (Springer-Verlag, Berlin, 1990).
[19] J. W. Johnston, Plasma Phys. **23**, 187 (1981).
[20] A. F. Almagri *et al.*, Phys. Fluids **B4**, 4080 (1992).
[21] H. Ji *et al.*, Phys. Rev. Lett. **73**, 668 (1994).
[22] H. Y. W. Tsui, Nucl. Fusion **28**, 1543 (1988).
[23] E. Hameiri and A. Bhattacharjee, Phys. Fluids **30**, 1743 (1987).
[24] L. Spitzer, Jr., *Physics of Fully Ionized Gases* (Interscience Publishers, New York, 1962), 2nd Ed., p. 28.